

Table 2. Radioactive counts of different fraction of silanized glass bound DNA undergoing Klenow synthesis

Sample	Count	Set 1 (cpm)	Set 2 (cpm)
Linear DNA	Total count	3096771.7	2511984
	Count left on glass	348369.25	370550.59
	TCA ppt.	88736.53	934446.8
	Stray count	1861045.8	1518335
	Incorporation (%)	28.7%	37.2%




Figure 1. A photographic print of the autoradiogram of a strip of nitrocellulose to which pUC18 DNA was Southern blotted. The nitrocellulose filter was hybridized with Klenow synthesized pUC18 DNA using flint glass-bound baked pUC18 DNA as template.

50 μ l bind silane (marketed by LKB). The treatment was carried out at 80°C for 20 min in the same eppendorf tube. Bind silane was removed as the supernatant after centrifugation and finally the silanized glass-bound baked DNA was used as substrate for generation of probes.

Glass-bound baked linearized pUC18 DNA was used as a template for synthesis reaction in a similar fashion as described above and the newly synthesized DNA was used as a probe to hybridized Southern blotted pUC18 DNA. Autoradiogram (Figure 2) of the strip of nitrocellulose filter showed the DNA synthesized is authentic pUC18 DNA.

We can conclude that DNA bound to flint glass is a good substrate for DNA polymerase. The advantage of using glass-baked DNA is that even sparingly available DNA samples once bound can be used repeatedly for the generation of probe DNA.

1. Rhodes, D and Klug, A, *Nature*, 1980, 286, 573.
2. Fodor, S. P. A., *et al*, *Science*, 1991, 251, 767.
3. Vogelstein, B. and Gillespie, D., *Proc. Natl. Acad. of Sci., USA*, 1979, 76, 615.

4. Sambrook, J., Fritsch, E. and Maniatis, T., *Molecular Cloning*, 2nd edn., Cold Spring Harbor Laboratory, New York, 1989.
5. Santra, C. R. and Thakur, A. R., *Int. J. Biolo. Macromolecules*, 1984, 6, 152.

ACKNOWLEDGEMENTS. We thank Prof. C. K. Dasgupta for critically reading the manuscript and Mr Abir Mukherjee for initiating us to the world of glass-bound DNA. We also thank the Department of Biotechnology and Council of Scientific and Industrial Research, New Delhi, for financial assistance.

Received 30 January 1992, revised accepted 21 February 1992

Triplex formation between d-CGCTCT and the self-complementary oligonucleotide d-CAATCTCGCGA-GATTG-spectroscopic investigations

Anup Madan and R. V. Hosur

Chemical Physics Group, Tata Institute of Fundamental Research, Homi Babha Road, Bombay 400 005, India

We report here studies on triple helix formation by mixed purine-pyrimidine strands with a view to explore the general potential of oligomeric triplex formation as a recognition phenomenon of DNA sequences. It is observed that the hexamer d-CGCTCT-3' with a purine at second position forms a stable triplex with a self-complementary DNA duplex d-CAATCTCGCGA-GATTG-3' in the pH range 5-7, in the presence of 2M NaCl. ¹H NMR spectra in H₂O solution under these conditions show the imino resonances belonging to the Hoogsteen base pairs in the triplex. Thermodynamic parameters for the triplex formation have been determined by UV spectroscopy.

The existence of triplexes in DNA and RNA has been known for over three decades¹. In the ensuing years a large number of investigators have used pyrimidine oligodeoxynucleotide triple helix formation to recognize extended purine sequences in double helical DNA²⁻¹². From X-ray-fibre diffraction studies it has been observed that the third strand in the triplex sits in the major groove of the duplex, formed by the other two strands, is held to it by Hoogsteen base pairs¹³⁻¹⁵. The base triplets T.(AT) and C⁺.(GC) thus formed are shown in Figure 1a. It may be noted that the latter requires the protonation of the cytosine residue and hence its formation is pH-dependent^{3,9,17}. Formation of the base triplets such as G.(GC) and A.(AT) have also been recently reported¹⁶. Homopyrimidine oligodeoxynucleotides attached to DNA-cleaving agents have been used to cut duplex DNA^{3,5}. Strobel *et al.*⁶ established the usefulness of such sequences as probes for chromosome mapping and as antisense DNA for

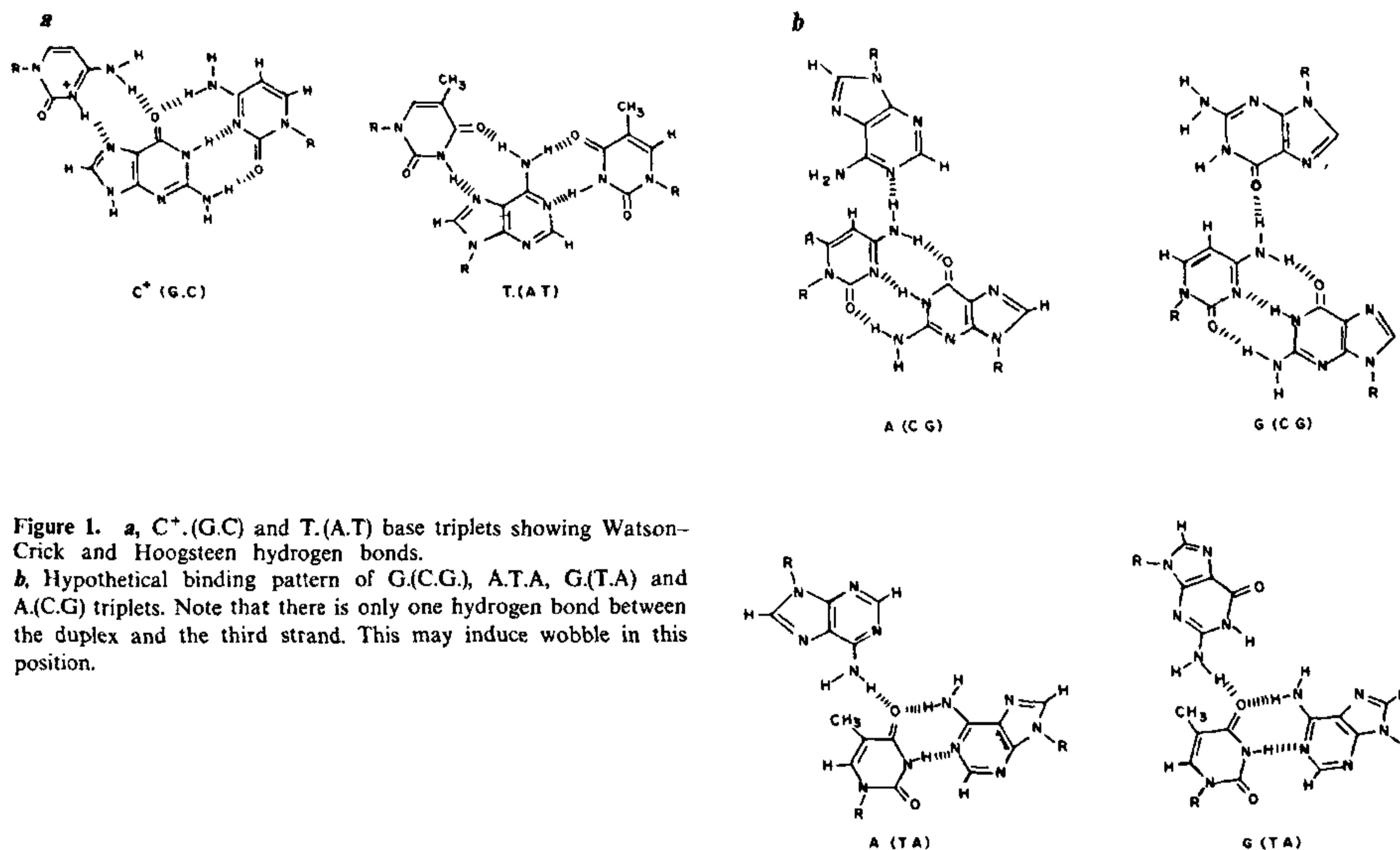


Figure 1. *a*, C⁺(G.C) and T.(A.T) base triplets showing Watson-Crick and Hoogsteen hydrogen bonds.

b, Hypothetical binding pattern of G.(C.G), A.(C.G), G.(T.A) and A.(TA) triplets. Note that there is only one hydrogen bond between the duplex and the third strand. This may induce wobble in this position.

chemotherapeutic application. However, the requirement of a homopyrimidine strand to bind a homopurine strand in the duplex for formation of the triplex appears as a limitation to the generality of the above application; in target DNA duplex, there could be breaks in a stretch of polypurine sequences by a pyrimidine base or vice versa and then the question arises whether such a stretch can still make triple helix. If a triplex can be formed, say G.(CG), A.(TA), G.(TA) or A.(CG) what will be the mode of interaction and what will be its stability? Figure 1,*b* shows likely binding pattern in such triplets. Possibility of G.(TA) has been predicted recently⁷. We have undertaken a systematic study to investigate these questions and in this paper we report triple helix formation by a hexamer stretch of polypyrimidine strand intercepted by a purine (G) at position 2, with a self-complementary 16 mer duplex containing the complementary sequence for the hexamer. UV absorbance spectroscopy has been used to determine the stoichiometry, stability, thermodynamics and melting behaviour of the oligomeric DNA triplex. ¹H NMR spectroscopy has been used to obtain finer details of the triple helix formation.

Oligodeoxyribonucleotide, d-CAATCTCGCGAGATTG (hereafter referred to as 16 mer) and d-CGCTCT (hereafter referred to as 6 mer) were synthesized on applied biosystems model 381A DNA synthesizer with β -cyanoethyl phosphoramidites. The purification was accomplished by reverse phase chromatography on a

LKB HPLC system using Applied Biosystems Polypore PRP column (7 × 250 mm)¹⁸. Concentrations of all oligomers were determined spectrophotometrically by monitoring OD at 260 nm, the following molar extinction coefficients (M⁻¹cm⁻¹) were used for different bases^{8,11}: 15,400 (A), 11,700 (G), 7300 (C), 8800 (T).

Unless indicated, all measurements were conducted in 50 mM sodium phosphate containing 1 mM EDTA and 2.0 M NaCl, at pH 5.5. The final pH was adjusted to the desired value using 0.1 M HCl or 0.1 M NaOH whenever necessary.

Stock solutions of the 16 mer and 6 mer (2.0 μ M) were prepared. To construct the mixing curve, 50–100 μ l of stock solution was added to a 1-cm path length quartz cuvette containing 600 μ l of stock solution of 16 mer duplex. After each addition, the contents were shaken well to ensure complete mixing followed by equilibration at 15°C for 15 min. After equilibration, the absorbance at 260 nm was measured. Mole fractions have been calculated using duplex concentration for 16mer and single strand concentration for 6 mer.

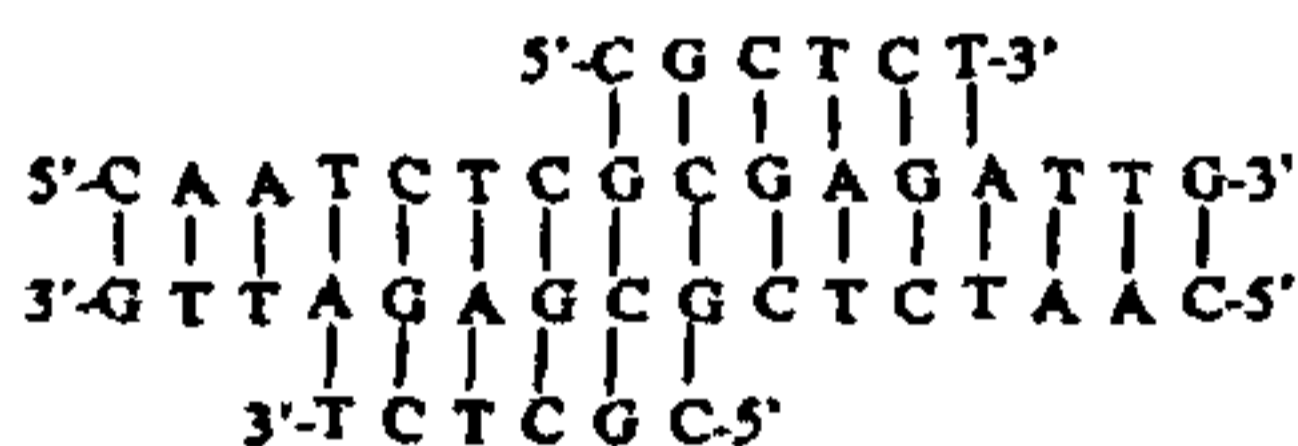
The 16 mer and 6 mer mixtures in stoichiometric proportions were heated to 80°C, cooled to room temperature slowly for proper annealing and then were filtered through 0.45- μ filter. The denaturation experiments were performed with such annealed complexes on a Shimadzu UV-2100 spectrophotometer. The

insulated cell compartment was heated from 15°C to 80°C using Shimadzu TCC-260 temperature controller and was allowed to equilibrate for 5 min after attaining each temperature. Samples were heated in 1-cm path length quartz cuvette. The thermal denaturation profiles have been represented as $d(A)/d(1/T)$ vs T plots and the temperature corresponding to the maximum in such a curve yields the transition temperature.

Proton NMR measurements in (90% H₂O + 10% ²H₂O) solution of the triplex were carried out on Bruker AM 500 MHz FT-NMR spectrometer in the temperature range 7°C to 35°C. The strong water signal was suppressed using the 1-1 pulse sequence.

Triplex formation

Figure 2 shows the UV mixing curve obtained by slow addition of the 6 mer to a constant volume of the 16 mer duplex. It is seen that at a mole fraction of 0.5, absorbance reaches a minimum and then starts increasing with further addition of the 6 mer solution. This indicates that the 16 mer duplex and the 6 mer single strand bind in 1:1 stoichiometry. Examination of the sequences of the 16 mer and 6 mer reveals that there are actually two sites at which 6 mer can bind its complementary sequence on the 16 mer duplex in a parallel fashion (Scheme 1).



Scheme 1.

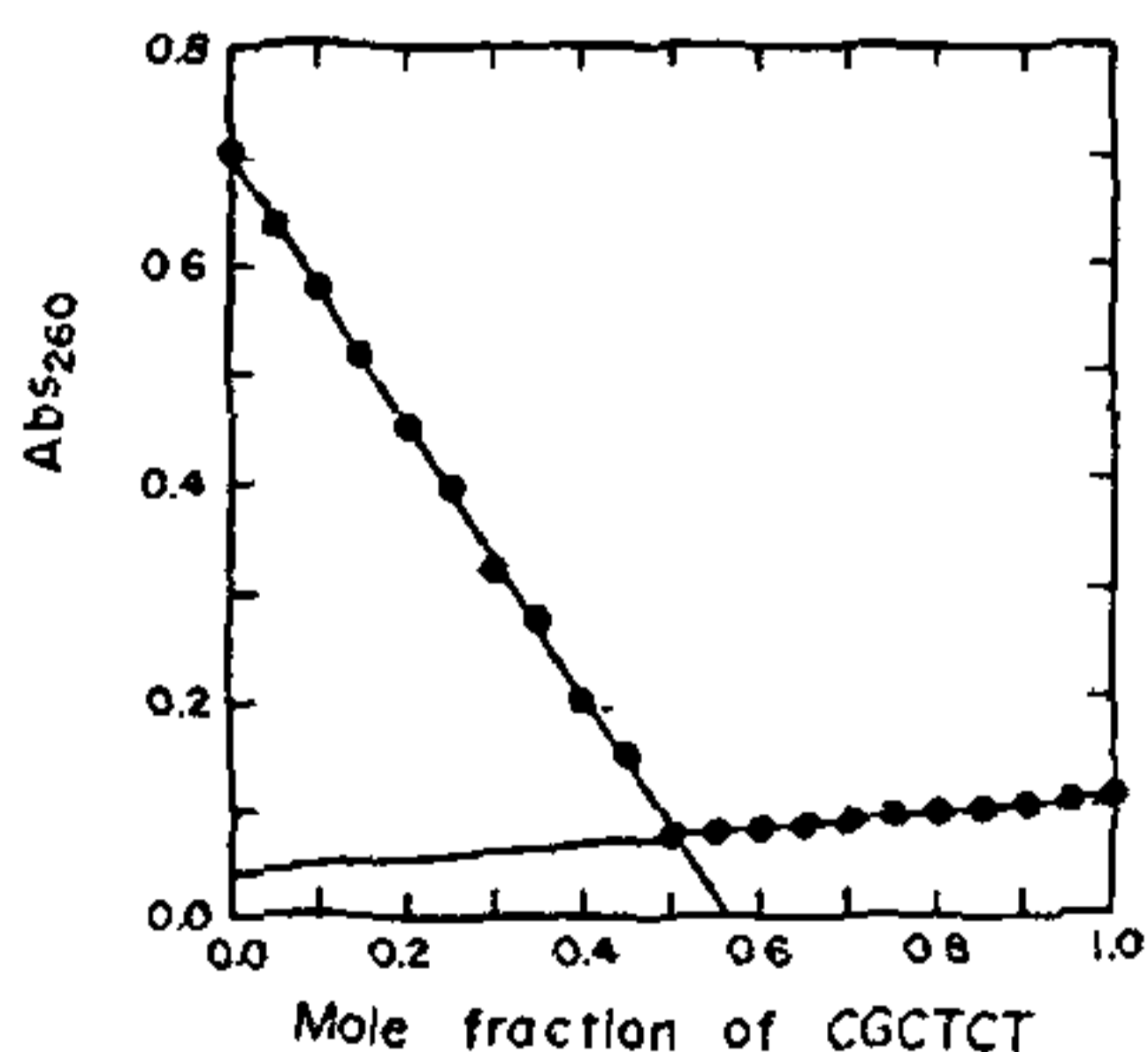


Figure 2. UV mixing curve for the reaction between d-CGCTCT and self-complementary duplex d-CAATCTCGCGAGATTG in 2.0 M NaCl, 1 mM ethylene diamine tetraacetic acid Na⁺ salt (EDTA), 50 mM sodium phosphate buffer, pH 5.5. Concentration of 16 mer is on double strand basis.

Such a binding would imply a 1:2 stoichiometry for the 16 mer duplex-6 mer interaction. Also the 5'-terminal two bases -CG- in the 6 mer would be involved in a two-step quadruplex formation. C.G.C.G. at step 1 and G.C.G.C. at step 2. However, observation of 1:1 stoichiometry of binding implies that such a complex is not formed and the complex is asymmetric.

Figure 3a shows the imino proton region of the 500 MHz ¹H NMR spectrum of the 16 mer duplex at 22°C, pH 7.0. Only seven peaks can be seen, indicating the duplex is symmetric, which must be expected owing to the self-complementary nature of the base sequence. Each peak accounts for two imino protons at equivalent positions from the two ends of the duplex. The terminal imino protons are not seen owing to rapid exchange of these protons with bulk water. In Figure 3,b, the imino proton resonance observed in triplex are shown as a function of temperature (7°C-35°C). It is obvious from the spectra that Watson-Crick pairing is intact in the entire range. But in addition, two new weak resonances are seen at 7°C and also at 15°C.

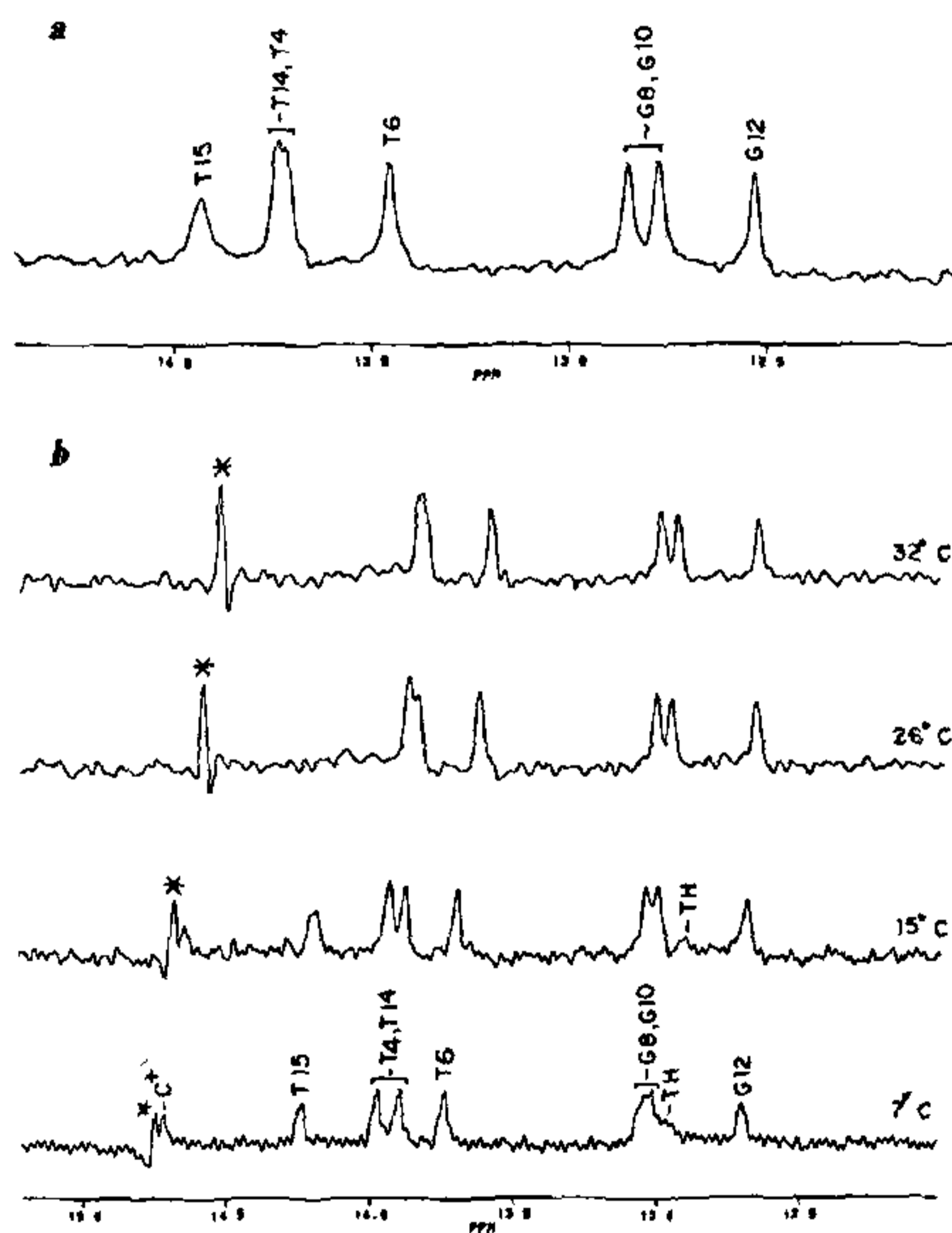


Figure 3. a, 500 MHz ¹H NMR spectrum showing imino proton region of the 16 mer duplex recorded at 22°C in H₂O solution containing 1.0 mM EDTA, 0.1 M NaCl, 50 mM sodium phosphate buffer, pH 7.0. b, Portion of the 500 MHz ¹H NMR spectrum of the triplex formed between self-complementary 16 mer duplex and d-CGCTCT in stoichiometric amounts at different temperatures in (90% H₂O and 10% ²H₂O) solution containing 2.0 M NaCl, 1 mM EDTA, 50 mM sodium phosphate buffer, pH 5.5. *, represents an artifact; C⁺ and TH refer to imino protons in Hoogsteen base pairs.

These must be attributed to the Hoogsteen base pairs C⁺-(G.C) and T-(A.T) between the hexamer and the 16 mer duplex. These are rather weak, implying high exchange rates with water as compared to Watson-Crick base pair. Further, the two resonances disappear at higher temperatures, namely 22°C and 35°C, which is consistent with the above conclusion. The pattern of chemical shifts of these peaks is the same as observed earlier^{19,20}. The downfield resonance may be assigned to C⁺ (NH) which must be expected to be deshielded because of the positive charge on the ring (see Figure 1,a). It is, however, difficult to quantify the intensities of these peaks and no conclusion about the number of protons in each peak can be drawn. Qualitatively, however, the C⁺ peak appears more intense than the T peak and this may be expected because of larger number of C⁺.G pairs in the triplex.

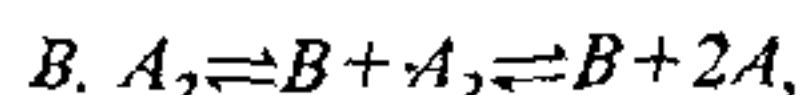
Figure 4,a shows the derivative melting curve of the triplex obtained by UV absorbance measurements at 260 nm at different temperatures²¹. Two transitions can be easily identified with maxima at 43±1°C and 70±1°C. The transition at lower temperature may be attributed to opening of the triplex into 6 mer single strand and 16 mer duplex and the other transition at the higher temperature is due to the melting of the duplex; the melting curve of the isolated duplex, which shows a single transition at 70±1°C, is plotted in Figure 4,b for comparison and identification of the two transitions of the triplex.

We have also studied the effect of pH on triplex formation and it is observed that increase in pH decreases the stability of the triplex and at pH 6.5, the first transition temperature drops to 35°C.

Thermodynamics of triple helix formation

The biphasic helix-coil transition of the triplex

represents the following equilibria



where B is 6mer and A₂ the 16mer duplex. Noting that one strand of duplex represents the purine strand, the other complementary strand represents the pyrimidine strand of the purine-pyrimidine triplexes considered by Pilch *et al.*²² their thermodynamic analysis can be extended to the present situation as well. The following two equations can be easily derived²²,

$$1/T_{\max}^H = (R/\Delta H^\circ) \ln C_A + (\Delta S^\circ - 0.188 R)/\Delta H^\circ \quad (1)$$

for Hoogsteen phases,

$$1/T_{\max}^W = (R/\Delta H^\circ) \ln C_A + (\Delta S^\circ + 0.468 R)/\Delta H^\circ \quad (2)$$

for W-C phases, where C_A is the concentration of 16 mer on duplex basis and T_{max}^H and T_{max}^W are the characteristic temperatures at which derivative curves show maxima, corresponding to the Hoogsteen and Watson-Crick phase respectively. R is the gas constant and ΔH° and ΔS° are the standard enthalpy change and standard entropy change respectively. (Note that T_{max} does not represent the usual melting temperature²².) Evidently plots of 1/T_{max}^H vs ln C_A enable determination of the thermodynamic parameters for the two processes.

Figure 5 shows such plots for the two processes described above. The linear correlation seen over the entire DNA concentration range studied suggests that both phases reflect bimolecular melting processes. Thermodynamic parameters derived from these plots are given in Table 1. The enthalpy change associated with the second transition of the triplex (-108.74 kcal mol⁻¹) is in excellent agreement with the enthalpy change for the disruption of the isolated duplex. This is

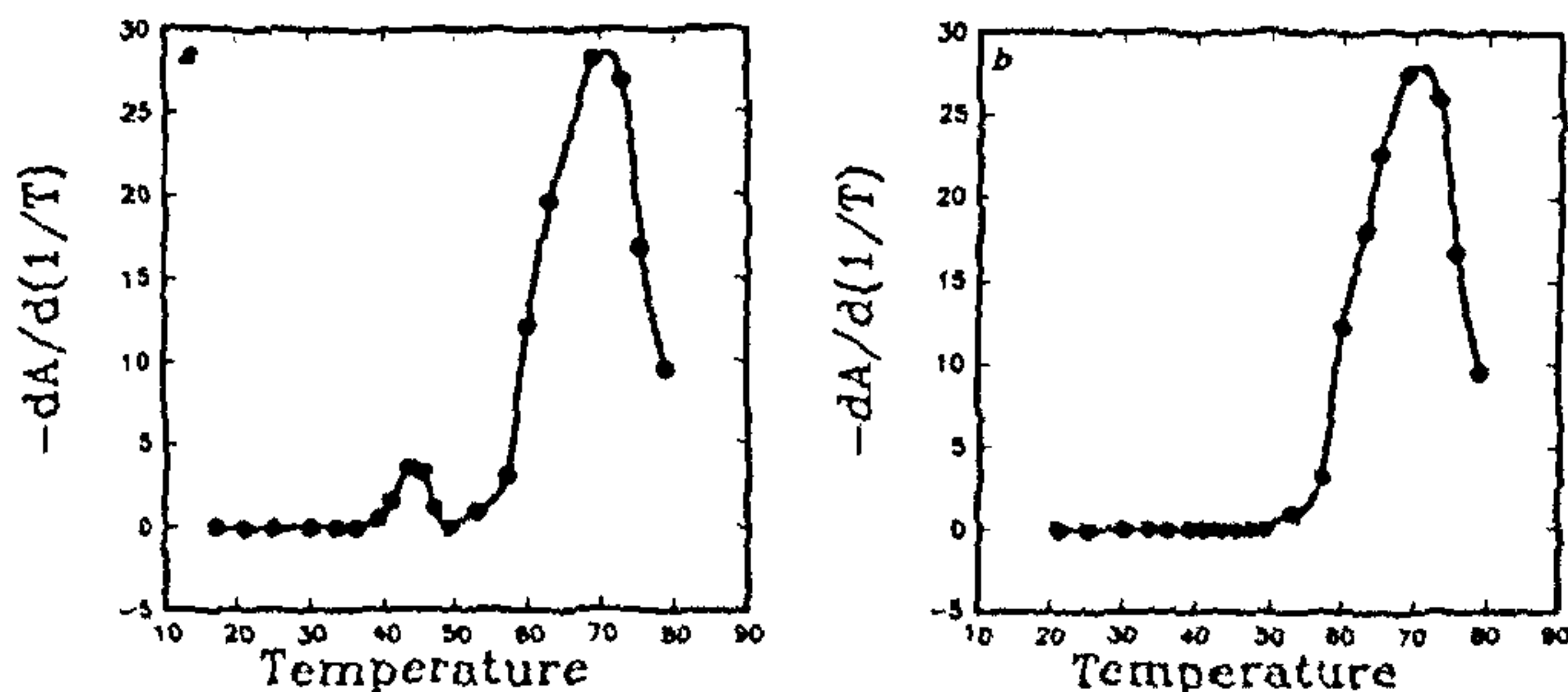


Figure 4. a, First derivative plot of the helix coil transitions in the triplex formed between self-complementary duplex d (CAATCTCGCGAGATTG) and the hexamer d (CGCTCT). b, First derivative plot of the helix coil transition in the self-complementary duplex d (CAATCTCGCGAGATTG).

Table 1. Thermodynamic parameters for the melting transitions of the triplex

Transition	T_{max} (°C)	ΔH° (kcal mol ⁻¹)	ΔS° (cal mol ⁻¹ deg ⁻¹)	ΔG° (kcal mol ⁻¹)	K (25°C) (M ⁻¹)
B A ₂ = B + A ₂	43.0	-23.8	-76.2	-1.14	6.9
B + A ₂ = B + 2A	69.0	-108.74	-315.67	-14.62	5.25 × 10 ¹⁰

* T_{max} at duplex concentration 4.2 μM.

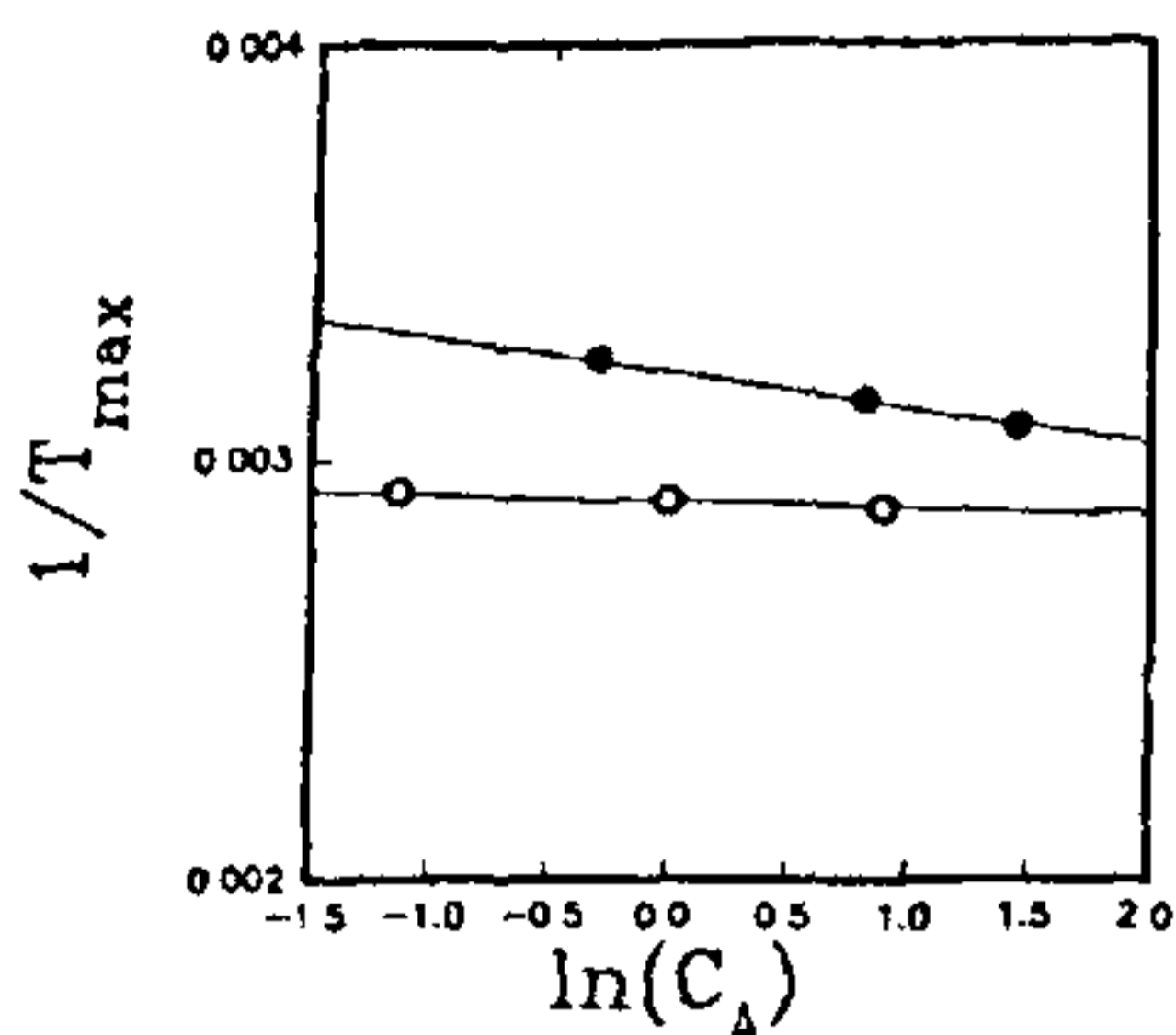


Figure 5. Plots of $1/T_M$ vs $\ln C_A$ of the triplex in 2.0 M NaCl, 1.0 mM EDTA, 50 mM sodium phosphate buffer, pH 5.5 for the Hoogsteen phase (●) and for the Watson-Crick phase (○). The concentration of the strands is in μmoles (duplex basis) and T_M is in the units of Kelvin.

also close to the predicted enthalpy change of -115.0 kcal mol⁻¹ calculated from the nearest neighbour analysis²³. Inspection of the ΔG° data also reveals that at 25°C and 2.0 M Na⁺, the triplex structure is only marginally stable ($\Delta G^\circ \approx -1.14$ kcal mol⁻¹) relative to significant stability of its host duplex ($\Delta G^\circ = -14.62$ kcal mol⁻¹). This is to be expected due to the short stretch of the triplex as compared to the length of the duplex molecule.

We have described here the formation of a triplex between a hexamer d-CGCTCT and a self-complementary duplex d-CAATCTCGGAGATTG and investigated the stability and thermodynamics of complex formation. It is significant that even for a hexamer stretch with one break, triplex formation is substantially favoured and the T_{max} temperature is as high as 44°C

at pH 5.5. For longer stretches the stability can be expected to be higher. This is of general interest for recognition between oligonucleotides and consequently in site-directed interactions in real systems.

1. Wells, R. D., Collier, D. A., Hanvey, J. C., Shimizu, M. and Wohlrab, F., *FASEB J.*, 1988, 2, 2939.
2. LeDoan, T. et al., *Nucleic Acids Res.*, 1987, 15, 7749.
3. Moser, H. E. and Dervan, P. B., *Science*, 1987, 238, 645.
4. Lyamichev, V. I., Mirkin, S. M., Frank-Kamenetski, M. D. and Cantor, C. R., *Nucleic Acids Res.*, 1988, 16, 2165.
5. Praseuth, D. et al., *Proc. Natl. Acad. Sci. USA*, 1988, 85, 1349.
6. Strobel, S. A., Moser, H. E. and Dervan, P. B., *J. Am. Chem. Soc.*, 1988, 110, 7927.
7. Griffin, L. C. and Dervan, P. B., *Science*, 1989, 245, 967.
8. Maker, L. J., Wold, B. and Dervan, P. B., *Science*, 1989, 245, 725.
9. Povsic, T. J. and Dervan, P. B., *J. Am. Chem. Soc.*, 1989, 111, 3059.
10. Strobel, S. A. and Dervan, P. B., *J. Am. Chem. Soc.*, 1989, 111, 7286.
11. Strobel, S. A. and Dervan, P. B., *Science*, 1990, 249, 73.
12. Sun J. S. et al., *Proc. Natl. Acad. Sci. USA*, 1989, 86, 9198.
13. Arnott, S. and Selsing, E., *J. Mol. Biol.*, 1974, 88, 509.
14. Arnott, S., Chandrasekaran, R., Hukins, D. W. L., Smith, P. J. C. and Watts, L., *J. Mol. Biol.*, 1974, 88, 523.
15. Arnott, S., Bond, P. J., Selsing, E. and Smith, P. J. C., *Nucleic Acids Res.*, 1976, 3, 2459.
16. Beal, P. A. and Dervan, P. B., *Science*, 1991, 251, 1360.
17. Lee, J. S., Johnson, D. A. and Morgan, A. R., *Nucleic Acids Res.*, 1979, 6, 3073.
18. Eadie, J. S., McBride, L. J., Efcavitch, J. W., Hoff, L. B. and Cathcart, R., *Anal. Biochem.*, 1987, 165, 442.
19. Rajagopal, P. and Feigon, J., *Nature*, 1989a, 339, 637.
20. Rajagopal, P. and Feigon, J., *Biochemistry*, 1989b, 28, 7859.
21. Gralla, J. and Crothers, D. M., *J. Mol. Biol.*, 1973, 78, 301.
22. Pilch, D. S., Brousseau, R. and Shafer, R. H., *Nucleic Acids Res.*, 1990a, 19, 5743.
23. Breslauer, K. J., Frank, R., Blöcker, H. and Marky, L. A., *Proc. Natl. Acad. Sci. USA*, 1986, 83, 3746.

Received 13 September 1991; revised accepted 26 February 1992